Green Chemistry

PAPER

Cite this: *Green Chem.*, 2014, **16**, 3881

Desulfurization of diesel fuel with nickel boride *in situ* generated in an ionic liquid†

Chenhua Shu, Tonghua Sun,* Qingbin Guo, Jinping Jia and Ziyang Lou

Received 17th April 2014,
Accepted 9th June 2014

DOI: 10.1039/c4gc00695j

www.rsc.org/greenchem

In order to improve the desulfurization efficiency, an ionic liquid (IL) was used as the solvent for the desulfurization of diesel fuel with nickel boride. The nickel boride prepared in IL–H_2O showed high specific surface area. The desulfurization efficiency of model organosulfur compounds in this work was higher than that in the previous studies. The desulfurization reactivity of model organosulfur compounds followed the order of BT (DBT) > 3-MBT > 4,6-DMDBT. Furthermore, the products of model organosulfur compounds after desulfurization were analyzed by GC/MS and their corresponding reaction routes were proposed. The effectiveness of nickel salts followed the order of $NiCl_2$ ($Ni(OAc)_2$) > $NiSO_4$ > $Ni(NO_3)_2$. The desulfurization efficiency of model diesel fuels reached 90.6% under the conditions of B/S molar ratio = 9, $Ni(OAc)_2$/S molar ratio = 3, oil/IL volume ratio = 3, water content in IL = 5%, and reaction time = 50 min. ILs maintained their original structures after regeneration. Finally, the desulfurization of real diesel fuel was carried out and a desulfurization efficiency of 88.6% was obtained in 50 min.

Introduction

SO_x emission from automobile exhausts not only pollutes air heavily, but also irreversibly poisons the metal catalysts in automobiles. So many countries have implemented stringent legislation to regulate the sulfur content of transportation fuels.[1,2] To meet the increasingly stringent environmental regulations, many deep desulfurization processes have been developed in the past few years such as alkylation,[3] extraction,[4–7] oxidation,[8–12] adsorption,[13–19] membrane separation,[20,21] and bio-desulfurization.[22] In addition, reductive desulfurization is also of importance both in the laboratory and in industry. Hydrodesulfurization (HDS), for example, is a traditional industrial process for sulfur removal from transportation fuels. However, HDS is not effective for removing heterocyclic sulfur compounds such as benzothiophene (BT), dibenzothiophene (DBT) and their derivatives.[1,2] Furthermore, it needs high investment and operating costs, and suffers from a significant loss in the octane number caused by saturation of olefins.[1,2]

Nickel boride, a fine, black solid that is easily prepared by the reduction of nickel salts with sodium borohydride ($NaBH_4$) in protic solvents, is a useful reducing agent for a variety of functional groups. Its low cost, easy preparation and handling, nonpyrophoric nature, and simple removal from a reaction mixture by filtration make it a particularly convenient reagent.[23] A lot of studies about the desulfurization of organosulfur compounds with nickel boride have also been carried out. For example, W. E. Truce *et al.* reported the desulfurization of mercaptans, sulfides and sulfoxides with nickel boride.[24] T. G. Back *et al.* used the nickel boride prepared with $NaBH_4$ and $NiCl_2$ to desulfurize BT and its derivatives (BTs), DBT and its derivatives (DBTs), alkylthio and arylthio compounds.[25,26] J. M. Khurana reported the desulfurization of thioureas, thiobarbiturates and dithiolanes with nickel boride.[27,28] However, the desulfurization efficiency is low for all the above studies. The reason for the low desulfurization efficiency can be explained from the desulfurization mechanism of nickel boride. According to the previous reports,[25,26,29] the desulfurization mechanism of nickel boride can be described as follows. An electron-rich state of nickel exists in nickel boride by transferring a part of electrons of boron to nickel, so the active hydrogen can be absorbed on the surface of nickel boride. Meanwhile, the organosulfur compounds also can be absorbed on the surface of nickel boride by complexation of their sulfur atoms with nickel boride. Then the active hydrogen and nickel on the surface of nickel boride would form a kind of nickel hydride intermediate. Finally, the oxidative addition of the C–S bond of organosulfur compounds to the nickel atom of the nickel hydride intermediate was followed by the reductive elimination of C–H, which resulted in the C–S bond cleavage. Based on this mechanism, it can be inferred that the high specific surface area of nickel boride can help to absorb active hydrogen and organosulfur compounds

School of Environmental Science and Engineering, Shanghai Jiaotong University, Dongchuan Road 800, Shanghai, 200240, People's Republic of China.
E-mail: sunth@sjtu.edu.cn

†Electronic supplementary information (ESI) available. See DOI: 10.1039/c4gc00695j

on the surface of nickel boride and accordingly increase the desulfurization efficiency. However, the solvents used in the previous studies were methanol, ethanol or methanol–tetrahydrofuran (THF) in which the nickel boride *in situ* generated easily agglomerated together to form larger clusters. Consequently, the generated nickel boride showed low specific surface area, which resulted in low desulfurization efficiency.

In this work, in order to improve the desulfurization efficiency, an ionic liquid (IL) was used as the solvent instead of methanol, ethanol or methanol–THF. The use of IL has several advantages. On the one hand, the nickel boride prepared in IL can be dispersed uniformly to form tiny particles. Furthermore, some ILs can be adsorbed on the surface of nickel boride by coordination reaction, which can stabilize the nickel boride by preventing its agglomeration.[30,31] Therefore, the nickel boride prepared in IL showed high specific surface area and will bring about high desulfurization efficiency. On the other hand, IL, an excellent extractant, can be used as an effective extractant in the desulfurization of fuel oils.[4–6] That is to say, IL will play two roles in the stabilization of nickel boride and extractive desulfurization during the course of desulfurization. Fig. 1 shows the present desulfurization process. Nickel boride is prepared with $NaBH_4$ and nickel salts (*e.g.* $4NaBH_4 + 2Ni(OAc)_2 + 9H_2O \rightarrow Ni_2B + 3H_3BO_3 + 4Na(OAc) + 12.5H_2$), and then the freshly prepared nickel boride is stabilized through coordination with IL. Simultaneously, the organosulfur compounds extracted from the oil phase and the active hydrogen coming from the hydrolysis of $NaBH_4$ ($NaBH_4 + H_2O \rightarrow NaBO_2 + H_2$) are also absorbed on the surface of nickel boride. Then the organosulfur compounds are desulfurized and transformed into the corresponding hydrocarbons. Finally, the produced hydrocarbons return to the oil phase due to its lessened polarity.

In the current study, we aim to investigate the effect of the use of IL on the desulfurization performance of nickel boride. Model and real diesel fuels were desulfurized with nickel boride prepared from nickel salts and $NaBH_4$. The IL 1-butyl-1-methylpyrrolidinium trifluoromethanesulfonate ([C_4mpyr][OTf]) and a small amount of H_2O was selected as the solvent. The nickel borides prepared in different solvents were characterized by transmission electron microscopy (TEM) and Fourier transform infrared spectrometry (FTIR). The desulfurization reactivity of different organosulfur compounds was investigated and their corresponding reaction routes were proposed. Furthermore, the effects of different nickel salts, the dosage of $NaBH_4$, the oil/IL volume ratio and the water content in IL on the desulfurization efficiency were also examined.

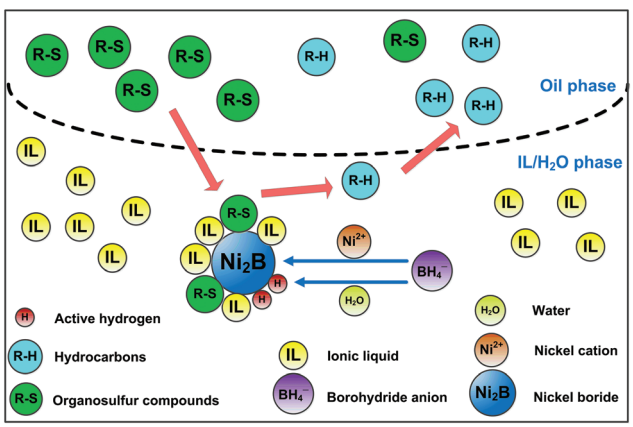

Fig. 1 Schematic diagram of the present desulfurization process.

Experimental section

Materials

Model diesel fuel with a sulfur content of 500 ppmw was prepared by dissolving BT, 3-methylbenzothiophene (3-MBT), DBT or 4,6-dimethyldibenzothiophene (4,6-DMDBT) in *n*-octane. Real diesel fuel with a sulfur content of 458 ppmw was supplied by Sinopec Shanghai Petrochemical Company. The IL [C_4mpyr][OTf] was prepared based on the previous paper.[32] The molecular structure of the IL and the nuclear magnetic resonance (NMR) spectra and spectroscopic data of the produced IL are given in the ESI.† BT, 3-MBT, DBT, 4,6-DMDBT and *n*-octane (AR) were purchased from Aladdin Reagent Co. Ltd (Shanghai, China). $NaBH_4$ (>96%), nickel acetate tetrahydrate ($Ni(OAc)_2{\cdot}4H_2O$, >98%, AR), nickel chloride hexahydrate ($NiCl_2{\cdot}6H_2O$, >98%, AR), nickel sulfate hexahydrate ($NiSO_4{\cdot}6H_2O$, >98%, AR) and nickel nitrate hexahydrate ($Ni(NO_3)_2{\cdot}6H_2O$, >98%, AR) were purchased from Sinopharm Chemical Reagent Co. Ltd (Shanghai, China).

Mutual solubility of the ionic liquid and real diesel fuel

The mutual solubility is an important factor in evaluating the applicability of an extractant because the noticeable solubility of ILs in diesel fuels may contaminate the fuel and further lead to possible NO_x pollution. On analyzing the IL-saturated real diesel fuels by high performance liquid chromatography (HPLC), no IL peak was found. Therefore, the IL [C_4mpyr][OTf] used here has negligible solubility in real diesel fuels. The solubility of real diesel fuels in ILs was measured using a gravimetric method by weighing the mass difference of a given amount of ILs and the corresponding ILs saturated with real diesel fuels. Results showed that the solubility of real diesel fuels in [C_4mpyr][OTf] was 4.3 wt%.

Desulfurization process

A typical desulfurization experiment was carried out in a two-neck flask. Model or real diesel fuels, IL and $NaBH_4$ were added into the two-neck flask in turn and the magnetic stirrer was turned on. A few minutes later, the nickel salts dissolved in H_2O were dripped into the two-neck flask slowly and the reaction began immediately. All desulfurization experiments were conducted at ambient temperature (10–30 °C) and pressure. The desulfurization efficiency was calculated by the following equation:

$$\text{Desulfurization efficiency (wt\%)} = \frac{TS_1 - TS_2}{TS_1} \times 100\% \quad (1)$$

where TS_1 is the sulfur content in the original diesel fuel sample and TS_2 is the sulfur content in the desulfurized diesel fuel sample.

Analytical methods

The structures of original and recycled ILs were analyzed by NMR (Bruker Avance III 400 NMR spectrometer). The IL-saturated real diesel fuel was analyzed by HPLC (Waters, C-18 column, 80/20 methanol–water mobile phase) equipped with a UV-Vis detector. The nickel borides prepared in different solvents were characterized by TEM (JEM-2010HT, 200KV) and FTIR (Nicolet-6700, using a thin KBr disc). The sulfur content in model diesel fuel after desulfurization was determined using a gas chromatography-flame ionization detector (GC-FID, GC-2010, Shimadzu) equipped with a DB-FFAP capillary column (0.25 mm × 30 m). Analysis conditions were as follows: the injector temperature was 340 °C and the detector temperature was 250 °C, and the column temperature was programmed from 100 °C to 300 °C (8 min) at 15 °C min^{-1}. The injection sample was 1 μl for all samples. The sulfur content in real diesel fuel was determined using a sulfur–nitrogen analyzer (Antek 9000, Antek). The data of the sulfur content for each sample were presented as the average of three replicates (data error <5%). The products of various model organosulfur compounds after desulfurization were analyzed using a gas chromatograph/mass spectrometer (GC/MS, 7890A-5975C, Agilent) equipped with a DB-5MS column (30 m × 0.25 mm × 0.25 μm). Helium was used as the carrier gas at a constant flow of 1 mL min^{-1}. The injector temperature was 270 °C and the oven temperature was programmed from 60 °C (5 min) to 300 °C at 20 °C min^{-1}. The split ratio was 200 : 1 and the injection sample was 0.1 μl for all samples. Mass spectrometry conditions were as follows: ionization voltage 70 eV; ion source temperature 230 °C; quadrupole temperature 150 °C; full scan mode in the *m*/*z* range 20–400. Compounds were identified by the use of National Institute of Standards and Technology (NIST) 2011 Library of Mass Spectra. The organosulfur compounds in original real diesel fuel and desulfurized real diesel fuel were analyzed by gas chromatography-flame photometric detection (GC-FPD, GC-2010, Shimadzu) with a DB-5MS capillary column (30 m × 0.32 mm × 0.25 μm). Analysis conditions were as follows: the injector temperature was 300 °C and the detector temperature was 250 °C, and the column temperature was programmed from 50 °C to 300 °C at 5 °C min^{-1}. The split ratio was 20 : 1 and the injection sample was 1 μl for all samples.

Results and discussion

Characterization of nickel boride

In order to study the effect of IL on the surface structure and stabilization of nickel boride, nickel borides were prepared in methanol, methanol–THF and IL–H_2O, respectively. The prepared nickel boride was washed with distilled water many times and dried under vacuum and then was characterized by TEM and FTIR. Fig. 2 shows the TEM images of nickel boride.

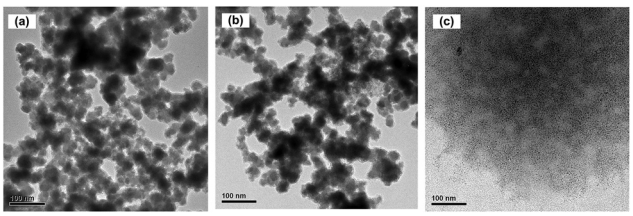

Fig. 2 TEM images of nickel borides prepared (a) in methanol, (b) in methanol–THF (3 : 1) and (c) in IL–H_2O.

It is obvious that the nickel borides prepared in methanol and in methanol–THF agglomerated together to form larger clusters whereas that prepared in IL–H_2O dispersed uniformly to form tiny particles. Therefore, the nickel boride prepared in IL–H_2O showed higher specific surface area compared with that prepared in methanol or methanol–THF. But why the nickel boride prepared in IL–H_2O did not agglomerate? It can be explained by the FTIR spectra of IL and nickel boride. Fig. 3a shows the FTIR spectra of [C_4mpyr][OTf]. The absorption peaks at 3036 cm^{-1}, 2968 cm^{-1} and 2880 cm^{-1} can be assigned to the stretching vibration (CH). 1633 cm^{-1} can be assigned to the stretching vibration (CC). 1471 cm^{-1} can be assigned to the scissoring vibration (CH_3). 1384 cm^{-1} can be assigned to the twisting vibration (CH_2). 1261 cm^{-1}, 1157 cm^{-1} and 1031 cm^{-1} can be assigned to the stretching vibration

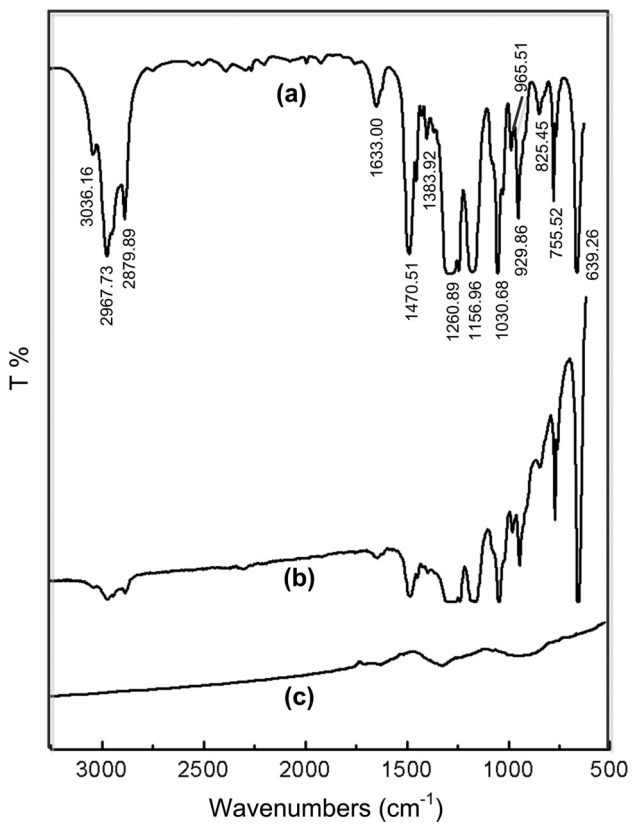

Fig. 3 FTIR spectra of (a) [C_4mpyr][OTf], (b) nickel boride prepared in IL–H_2O and (c) nickel boride prepared in methanol.

(SO_2 and CF). 966 cm^{-1}, 930 cm^{-1} and 825 cm^{-1} can be assigned to the vibration of the pyrrolidinium ring. 756 cm^{-1} and 639 cm^{-1} can be assigned to the scissoring vibration (CF_3 and OSO).[33,34] All these peaks confirm the structure of [C_4mpyr][OTf]. Fig. 3b shows the FTIR spectra of the nickel boride prepared in IL–H_2O. It is obvious that the nickel boride prepared in IL–H_2O has the same characteristic absorption peaks as the IL, which indicates that some IL still remained on the surface of nickel boride though nickel boride was washed with distilled water many times. However, [C_4mpyr][OTf] is miscible with water and can be washed off with distilled water. Furthermore, the characteristic absorption peaks of IL could not be observed in the spectra of nickel boride prepared in methanol (Fig. 3c). Therefore, it can be inferred that IL was combined with nickel boride by some strong chemical bonds instead of simple physical adsorption. In addition, according to the previous studies,[30,31] the [C_4mpyr] cation in IL can coordinate with nickel boride through the lone pair electrons of functional groups on them, so the chemical bonds should be coordinate bonds.

The results of TEM and FTIR indicated that the nickel boride prepared in IL–H_2O showed higher specific surface area because its agglomeration was prevented through coordinating with IL. High specific surface area can help to absorb active hydrogen and organosulfur compounds on the surface of nickel boride and accordingly improve the desulfurization efficiency.

Desulfurization of different organosulfur compounds

To investigate the effectiveness of the present process for different organosulfur compounds in diesel fuel, the desulfurization efficiency of four model organosulfur compounds such as BT, 3-MBT, DBT and 4,6-DMDBT was tested under similar conditions. Fig. 4 shows the desulfurization efficiency of four model organosulfur compounds. Higher desulfurization efficiency was obtained for all the model organosulfur compounds compared with that in the previous studies,[25,26] *e.g.* the desulfurization efficiency of BT increased from 82% (in the previous studies) to 98% (in this work), the desulfurization efficiency of DBT increased from 83% (in the previous studies) to 97% (in this work) and the desulfurization efficiency of 4,6-DMDBT increased from 29% (in the previous studies) to 72% (in this work). These results indicated that the use of IL really improved the desulfurization efficiency. The desulfurization efficiency of DBT was almost equal to that of BT. But the desulfurization efficiency of 4,6-DMDBT was much less than that of BT and DBT. The desulfurization reactivity of model organosulfur compounds followed the order of BT (DBT) > 3-MBT > 4,6-DMDBT. This result showed that the desulfurization reactivity is significantly affected by steric hindrance. On the other hand, the products of various model organosulfur compounds after desulfurization were analyzed by GC/MS and their corresponding reaction routes were proposed. As shown in Fig. 5, the reaction routes consisted of direct desulfurization (DDS) and hydrogenation (HYD). The detailed reaction routes of various model organosulfur compounds were as follows: (i) BT was transformed into ethylbenzene (EB) by DDS; (ii) 3-MBT was transformed into isopropylbenzene (IPB) by DDS; (iii) the desulfurization of DBT proceeded by DDS and HYD. The DDS route proceeded over direct cleavage of the C–S bond of DBT to biphenyl (BP), followed by hydrogenation to cyclohexylbenzene (CHB). The HYD route proceeded over hydrogenation of DBT to tetrahydrodibenzothiophene (THDBT) and hexahydrodibenzothiophene (HHDBT), followed by cleavage of the C–S bond to CHB; (iv) the desulfurization of 4,6-DMDBT also proceeded by DDS and HYD. The DDS route proceeded over direct cleavage of the C–S bond of 4,6-DMDBT to 3,3′-dimethylbiphenyl (3,3′-DMBP), followed by hydrogenation to 3,3′-dimethylcyclohexylbenzene (3,3′-DMCHB). The HYD route proceeded over hydrogenation of 4,6-DMDBT to 4,6-dimethyltetrahydrodibenzothiophene (4,6-DM-TH-DBT) and 4,6-dimethylhexahydrodibenzothiophene (4,6-DM-HHDBT), followed by cleavage of the C–S bond to 3,3′-DMCHB. These results are almost in agreement with the previous reports.[35–40]

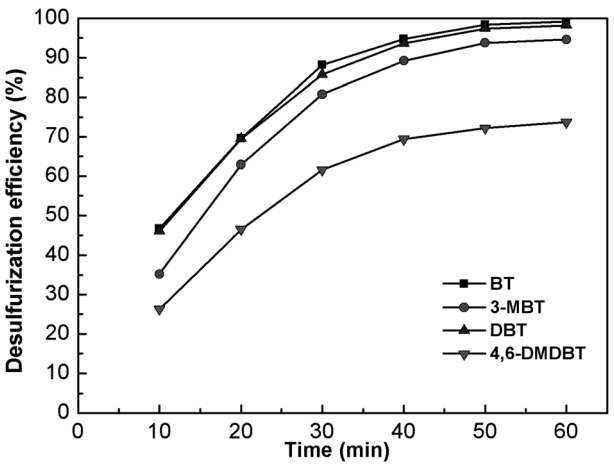

Fig. 4 Desulfurization efficiency of BT, 3-MBT, DBT and 4,6-DMDBT. Conditions: various model diesel fuels with sulfur contents of 500 ppmw were prepared by dissolving BT, 3-MBT, DBT or 4,6-DMDBT in *n*-octane, respectively. B/S molar ratio = 9, $Ni(OAc)_2$/S molar ratio = 3, oil/IL volume ratio = 3, and water content in IL = 5%.

Effect of nickel salts

The surface structure of nickel boride varied with preparation methods. There are three forms of nickel – nickel metal, nickel oxide and boron bound nickel – on the surface of nickel boride, but only the boron bound nickel plays a key role in the desulfurization of organosulfur compounds.[41] Furthermore, different precursors of nickel salts used will result in different proportions of surface nickels and accordingly affect the desulfurization activity of nickel boride. Fig. 6 shows the desulfurization efficiency of model organosulfur compounds by different nickel salts. As shown in Fig. 6, the desulfurization efficiency is high for any organosulfur compounds when $NiCl_2$ and $Ni(OAc)_2$ were used as the precursors of nickel salts, whereas the desulfurization efficiency is low when $Ni(NO_3)_2$ was used. The effectiveness of nickel salts followed the order of $NiCl_2$ ($Ni(OAc)_2$) > $NiSO_4$ > $Ni(NO_3)_2$. According to the previous reports,[41] more boron bound nickel could be obtained

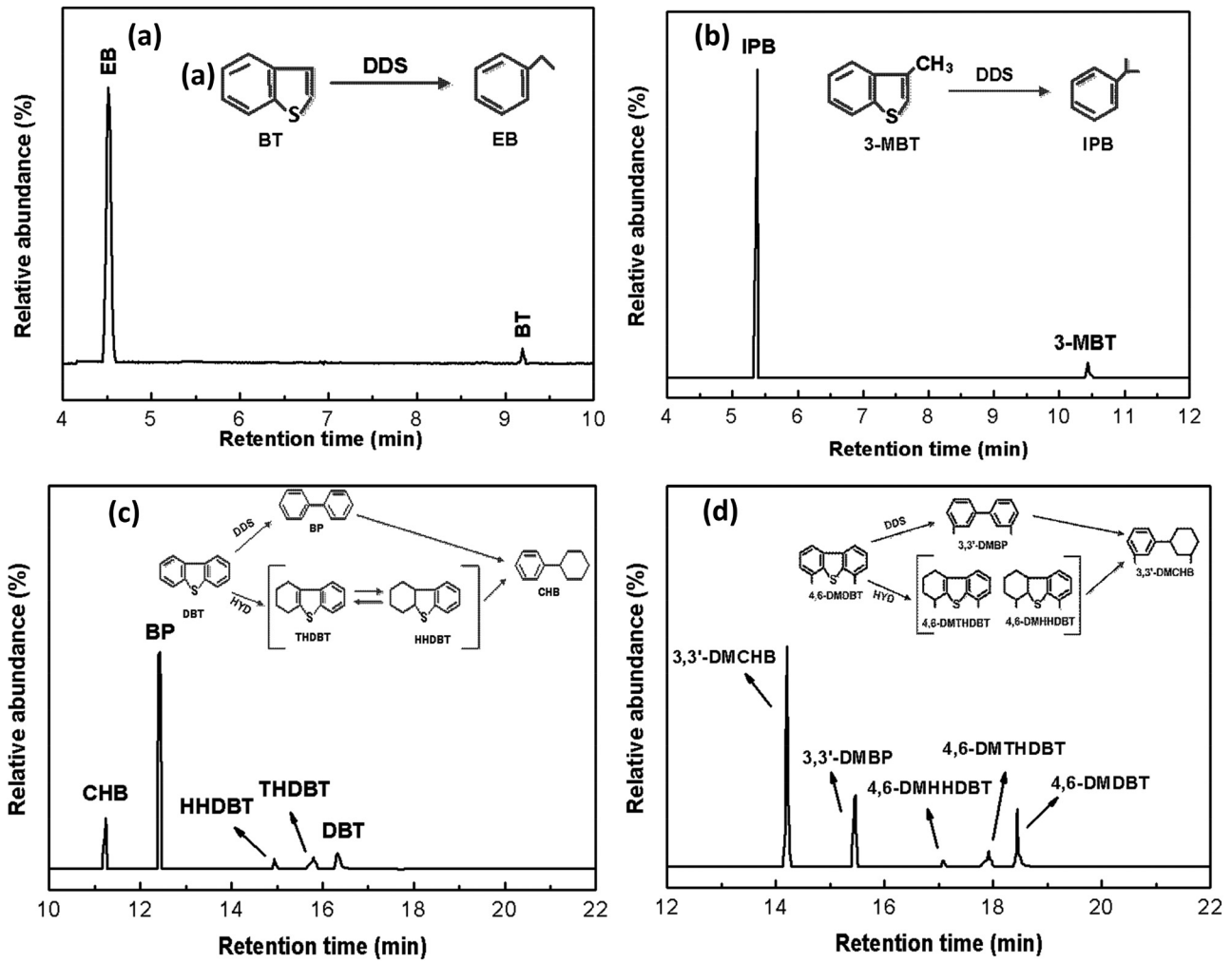

Fig. 5 GC/MS spectra of (a) BT, (b) 3-MBT, (c) DBT and (d) 4,6-DMDBT after desulfurization and their corresponding reaction routes. Conditions: various model diesel fuels with a sulfur content of 500 ppmw were prepared by dissolving BT, 3-MBT, DBT or 4,6-DMDBT in *n*-octane, respectively. B/S molar ratio = 9, $Ni(OAc)_2$/S molar ratio = 3, oil/IL volume ratio = 3, water content in IL = 5%, and reaction time = 50 min.

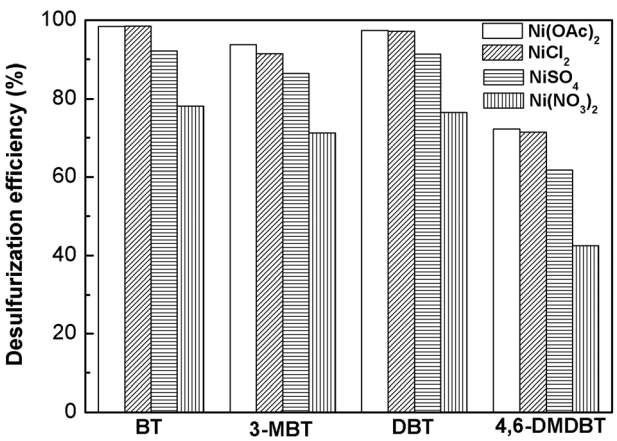

Fig. 6 Effect of different nickel salts on the desulfurization efficiency. Conditions: various model diesel fuels with a sulfur content of 500 ppmw were prepared by dissolving BT, 3-MBT, DBT or 4,6-DMDBT in *n*-octane, respectively. B/S molar ratio = 9, Ni/S molar ratio = 3, oil/IL volume ratio = 3, water content in IL = 5%, and reaction time = 50 min.

on the surface of nickel boride when $NiCl_2$ or $Ni(OAc)_2$ was used as the precursors of nickel salts. Therefore, this result is in agreement with the previous reports.[41] On the other hand, the effect of the dosage of nickel salt on the desulfurization efficiency was also investigated taking $Ni(OAc)_2$ for example. As shown in Fig. 7, the desulfurization efficiency increased with the increasing $Ni(OAc)_2$/sulfur ($Ni(OAc)_2$/S) molar ratio in the same reaction time, *e.g.* the desulfurization efficiency increased from 60.6% at a $Ni(OAc)_2$/S molar ratio = 1 to 90.6% at a $Ni(OAc)_2$/S molar ratio = 3 in 50 min. However, when the $Ni(OAc)_2$/S molar ratio was more than 3 the desulfurization efficiency remained almost stable.

Effect of $NaBH_4$

$NaBH_4$ plays a dual role in the desulfurization process. On the one hand, it reacts with nickel salts to obtain nickel boride. On the other hand, its hydrolysis produces a large amount of active hydrogen. So it is very necessary to investigate the effect of the dosage of $NaBH_4$ on the desulfurization efficiency. Fig. 8

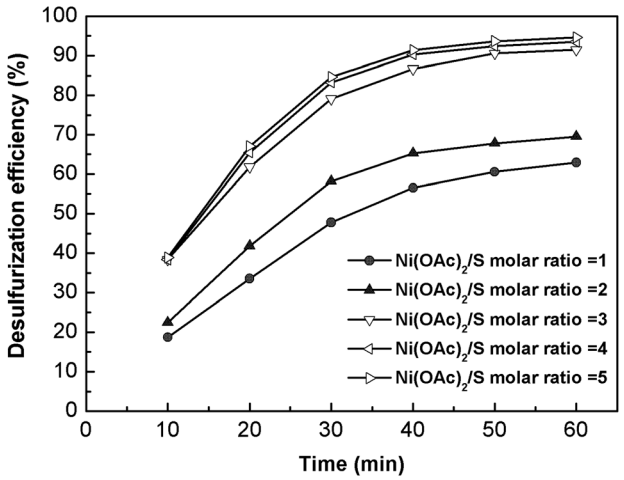

Fig. 7 Effect of $Ni(OAc)_2$/S molar ratio on the desulfurization efficiency. Conditions: model diesel fuels with a sulfur content of 500 ppmw were prepared by dissolving an equal molar amount of BT, 3-MBT, DBT and 4,6-DMDBT in *n*-octane. B/S molar ratio = 9, oil/IL volume ratio = 3, and water content in IL = 5%.

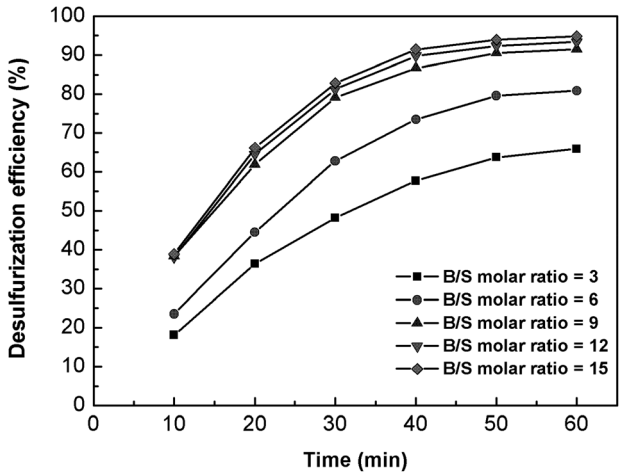

Fig. 8 Effect of B/S molar ratio on the desulfurization efficiency. Conditions: model diesel fuels with a sulfur content of 500 ppmw were prepared by dissolving an equal molar amount of BT, 3-MBT, DBT and 4,6-DMDBT in *n*-octane. $Ni(OAc)_2$/S molar ratio = 3, oil/IL volume ratio = 3, and water content in IL = 5%.

shows the effect of $NaBH_4$/sulfur (B/S) molar ratio on the desulfurization efficiency. The desulfurization efficiency increased rapidly with the increase of reaction time initially, and then increased slowly for any B/S molar ratio. Furthermore, the desulfurization efficiency increased with the increase of B/S molar ratio in the same reaction time, *e.g.* the desulfurization efficiency increased from 63.7% at a B/S molar ratio = 3 to 90.6% at a B/S molar ratio = 9 in 50 min. However, the desulfurization efficiency increased negligibly when the B/S molar ratio was more than 9. So the B/S molar ratio of 9 was used in this work.

Effect of the oil/IL volume ratio

Fuel oil and IL are immiscible, so the mass transfer between oil and IL can affect the desulfurization efficiency. As shown in Fig. 9, the desulfurization efficiency increased with the decrease of oil/IL volume ratio in the same reaction time, *e.g.* the desulfurization efficiency increased from 61.2% at an oil/IL volume ratio = 5 to 90.6% at an oil/IL volume ratio = 3 in 50 min. The reason is probably that the increase of IL volume can enhance the transfer of organosulfur compounds from the oil phase to the IL phase, which increases the reaction rate. Furthermore, the total water mass increases with the increase of IL volume when the water content in IL is constant, which favors the hydrolysis of $NaBH_4$ and the preparation of nickel boride, accordingly the desulfurization efficiency increases. However, the desulfurization efficiency increased negligibly when the oil/IL volume ratio was less than 3. So the oil/IL volume ratio of 3 was chosen in this work.

Effect of the water content in IL

There are two contradictory effects observed by increasing the water content in IL. On the one hand, it is well known that a protic solvent (*e.g.* water) is necessary for the hydrolysis of $NaBH_4$ and for the preparation of nickel boride.[23] On the other hand, increasing water content in IL can decrease the sulfur partition coefficient between IL and oil,[42–44] which lowers the extractive ability of IL for organosulfur compounds from the oil phase and accordingly decreases the desulfurization efficiency. So it is necessary to investigate a reasonable water content in IL for the desulfurization process. As shown in Fig. 10, the desulfurization efficiency increased initially, and then decreased with the increase of water content in IL. The maximum value of desulfurization efficiency was obtained when the water content in IL was 5%.

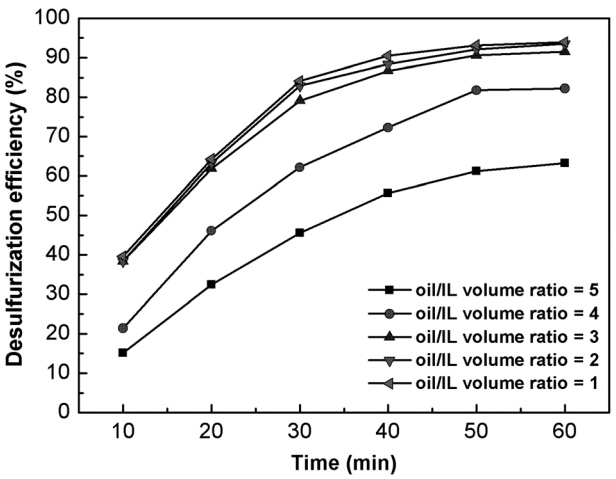

Fig. 9 Effect of oil/IL volume ratio on the desulfurization efficiency. Conditions: model diesel fuels with a sulfur content of 500 ppmw were prepared by dissolving an equal molar amount of BT, 3-MBT, DBT and 4,6-DMDBT in *n*-octane. B/S molar ratio = 9, $Ni(OAc)_2$/S molar ratio = 3, and water content in IL = 5%.

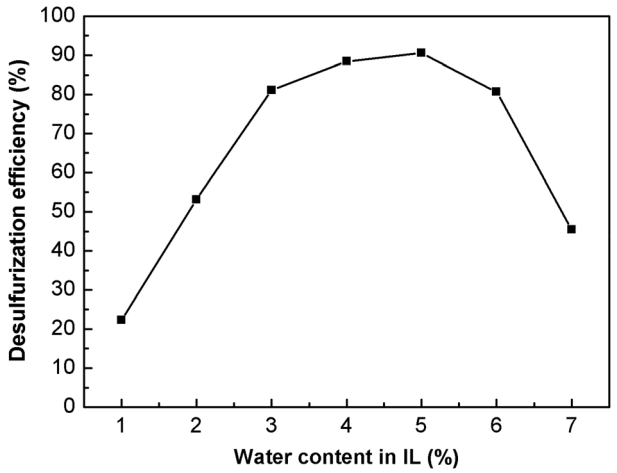

Fig. 10 Effect of water content in IL on the desulfurization efficiency. Conditions: model diesel fuels with a sulfur content of 500 ppmw were prepared by dissolving an equal molar amount of BT, 3-MBT, DBT and 4,6-DMDBT in *n*-octane. B/S molar ratio = 9, $Ni(OAc)_2$/S molar ratio = 3, oil/IL volume ratio = 3, reaction time = 50 min.

Recycling of the ionic liquid

For the industrial application of ILs, the regeneration and subsequent recycling of ILs are of vital importance. In this work, the IL [C_4mpyr][OTf] is miscible with water, so the used IL can be regenerated by mixing it with an equal volume of water to remove the residual diesel fuel in IL and then distillation at 110 °C. The structures of original and recycled ILs were analyzed by NMR (ESI, Fig. S1–S3†). The ^{1}H, ^{13}C and ^{19}F NMR spectra of the recycled ILs were nearly similar to that of the original ILs, which indicated that the ILs maintained their original structures after regeneration. On the other hand, the desulfurization performance of the recycled ILs was also investigated and the result is shown in Fig. 11. The desulfurization efficiency suffered from a slight decrease after every recycle and dropped from 90.6% to 87.5% after 8 recycles. The possible reason was that some IL was lost during the course of desulfurization and regeneration.

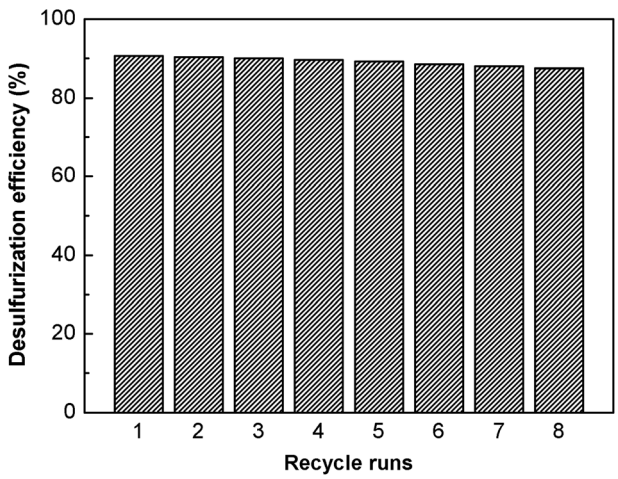

Fig. 11 Effect of recycle runs of IL on the desulfurization efficiency. Conditions: model diesel fuels with a sulfur content of 500 ppmw were prepared by dissolving an equal molar amount of BT, 3-MBT, DBT and 4,6-DMDBT in *n*-octane. B/S molar ratio = 9, $Ni(OAc)_2$/S molar ratio = 3, oil/IL volume ratio = 3, water content in IL = 5%, and reaction time = 50 min.

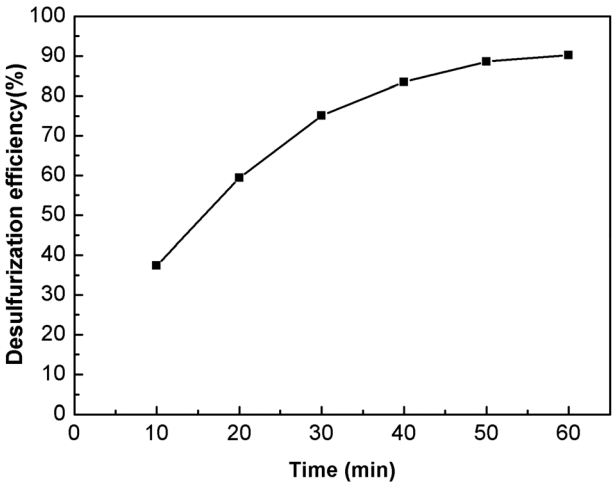

Fig. 12 Effect of reaction time on the desulfurization efficiency for real diesel fuel. Conditions: B/S molar ratio = 9, $Ni(OAc)_2$/S molar ratio = 3, oil/IL volume ratio = 3, and water content in IL = 5%.

Desulfurization of real diesel fuel

The desulfurization performance of the present process for real diesel fuel was also investigated. Fig. 12 shows the effect of reaction time on the desulfurization efficiency for real diesel fuel. The desulfurization efficiency increased with the increasing reaction time when the reaction time was less than 50 min and then remained almost constant even though the reaction time continued increasing. The effect of reaction time on the desulfurization efficiency for real diesel fuel was similar to that for model diesel fuel (as shown in Fig. 7 and 8). However, a desulfurization efficiency of 88.6% was obtained for real diesel fuel, which was somewhat lower than that for model diesel fuel. The reason was probably that real diesel fuel contained more complex components. On the other hand, the organosulfur compounds in the original real diesel fuel and desulfurized real diesel fuel were analyzed by GC-FPD. As shown in Fig. 13, most of organosulfur compounds in real diesel fuel were desulfurized except a small amount of BTs and DBTs containing alkyl substituents. This result further proves that the desulfurization reactivity of organosulfur compounds is significantly affected by steric hindrance, which is consistent with the above result.

Conclusions

In this work, a novel process for the desulfurization of diesel fuel was presented with nickel boride *in situ* generated in an ionic liquid. The IL [C_4mpyr][OTf] has negligible solubility in real diesel fuels whereas the solubility of real diesel fuels in [C_4mpyr][OTf] was 4.3 wt%. The nickel borides prepared in

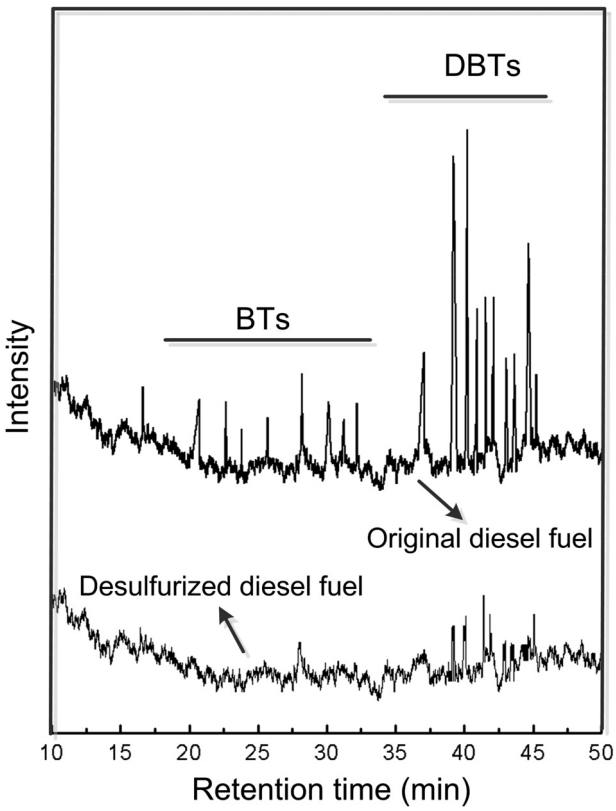

Fig. 13 GC-FPD chromatograms of original real diesel fuel and desulfurized real diesel fuel. Conditions: B/S molar ratio = 9, $Ni(OAc)_2$/S molar ratio = 3, oil/IL volume ratio = 3, water content in IL = 5%, and reaction time = 50 min.

different solvents were characterized by TEM and FTIR. Results showed that IL was combined with nickel boride by some strong chemical bonds and the nickel boride prepared in IL–H_2O showed high specific surface area. The desulfurization reactivity of organosulfur compounds followed the order of BT (DBT) > 3-MBT > 4,6-DMDBT, which indicated that the desulfurization reactivity is significantly affected by steric hindrance. The effectiveness of nickel salts followed the order of $NiCl_2$ ($Ni(OAc)_2$) > $NiSO_4$ > $Ni(NO_3)_2$. Under the conditions of B/S molar ratio = 9, $Ni(OAc)_2$/S molar ratio = 3, oil/IL volume ratio = 3, water content in IL = 5%, reaction time = 50 min, the desulfurization efficiency reached 90.6% for model diesel fuels. ILs maintained their original structures after regeneration and the desulfurization efficiency dropped from 90.6% to 87.5% after 8 recycles. Finally, the desulfurization performance of the present process for real diesel fuel was investigated and a desulfurization efficiency of 88.6% was obtained in 50 min. Based on the result of GC-FPD, most of the organosulfur compounds in real diesel fuel were desulfurized except a small amount of BTs and DBTs containing alkyl substituents. This work indicated that higher desulfurization efficiency could be obtained by introducing IL as the solvent in the desulfurization of diesel fuel with nickel boride, which will propel the commercial application of the desulfurization of diesel fuel with nickel boride.

Acknowledgements

This work was financially supported by the National Natural Science Foundation of China (no. 21377083), the National Natural Science Foundation of China (no. 41173108) and SMC-New Artist Scholar Award Plan (B) by Shanghai Jiaotong University (2011).

References

1 P. S. Kulkarni and C. A. M. Afonsoa, *Green Chem.*, 2010, **12**, 1139–1149.
2 V. C. Srivastava, *RSC Adv.*, 2012, **2**, 759–783.
3 R. Wang, Y. H. Li, B. S. Guo and H. W. Sun, *Energy Fuels*, 2011, **25**, 3940–3949.
4 J. J. Gao, H. Meng, Y. Z. Lu, H. X. Zhang and C. X. Li, *AIChE J.*, 2013, **59**, 948–958.
5 Y. Nie, C. X. Li and Z. Wang, *Ind. Eng. Chem. Res.*, 2007, **46**, 5108–5112.
6 X. C. Jiang, Y. Nie, C. X. Li and Z. H. Wang, *Fuel*, 2008, **87**, 79–84.
7 C. P. Li, D. Li, S. S. Zou, Z. Li, J. M. Yin, A. L. Wang, Y. N. Cui, Z. L. Yao and Q. Zhao, *Green Chem.*, 2013, **15**, 2793–2799.
8 Y. X. Ding, W. S. Zhu, H. M. Li, W. Jiang, M. Zhang, Y. Q. Duan and Y. H. Chang, *Green Chem.*, 2011, **13**, 1210–1216.
9 H. X. Zhang, J. J. Gao, H. Meng, Y. Z. Lu and C. X. Li, *Ind. Eng. Chem. Res.*, 2012, **51**, 4868–4874.
10 W. S. Zhu, P. W. Wu, L. Yang, Y. H. Chang, Y. H. Chao, H. M. Li, Y. Q. Jiang, W. Jiang and S. H. Xun, *Chem. Eng. J.*, 2013, **229**, 250–256.
11 W. Zhang, H. Zhang, J. Xiao, Z. X. Zhao, M. X. Yu and Z. Li, *Green Chem.*, 2014, **16**, 211–220.
12 H. Y. Lü, C. L. Deng, W. Z. Ren and X. Yang, *Fuel Process. Technol.*, 2014, **119**, 87–91.
13 R. T. Yang, H. J. Hernández-Maldonado and F. H. Yang, *Science*, 2003, **301**, 79–81.
14 A. J. Hernández-Maldonado and R. T. Yang, *J. Am. Chem. Soc.*, 2004, **126**, 992–993.
15 L. F. Wang, R. T. Yang and C. L. Sun, *AIChE J.*, 2013, **59**, 29–32.
16 J. Xiao, X. X. Wang, M. Fujii, Q. J. Yang and C. S. Song, *AIChE J.*, 2013, **59**, 1441–1445.
17 N. A. Khan and S. H. Jhung, *J. Hazard. Mater.*, 2013, **260**, 1050–1056.
18 S. Dasgupta, P. Gupta, Aarti, A. Nanoti, A. N. Goswami, M. O. Garg, E. Tangstad, Ø. B. Vistad, A. Karlsson and M. Stöcker, *Fuel*, 2013, **108**, 184–189.
19 M. Seredych and T. J. Bandosz, *Appl. Catal., B*, 2011, **106**, 133–141.
20 L. G. Lin, Y. Z. Zhang and Y. Kong, *Fuel*, 2009, **88**, 1799–1809.
21 H. R. Mortaheb, F. Ghaemmaghami and B. Mokhtarani, *Chem. Eng. Res. Des.*, 2012, **90**, 409–432.

22 Y. F. Hou, Y. Kong, J. R. Yang, J. H. Zhang, D. Q. Shi and W. Xin, *Fuel*, 2005, **84**, 1975–1979.
23 J. M. Khurana and A. Gogia, *Org. Prep. Proced. Int.*, 1997, **29**, 1–32.
24 W. E. Truce and F. M. Perry, *J. Org. Chem.*, 1965, **30**, 1316–1317.
25 T. G. Back, J. K. Yang and H. R. Krouse, *J. Org. Chem.*, 1992, **57**, 1986–1990.
26 T. G. Back, D. L. Baron and K. Yang, *J. Org. Chem.*, 1993, **58**, 2407–2413.
27 J. M. Khurana and G. Kukreja, *J. Heterocycl. Chem.*, 2003, **40**, 677–679.
28 J. M. Khurana and D. Magoo, *Synth. Commun.*, 2010, **40**, 2908–2913.
29 C. H. Shu, T. H. Sun, H. B. Zhang, J. P. Jia and Z. Y. Lou, *Fuel*, 2014, **121**, 72–78.
30 B. J. Liaw, S. J. Chiang, C. H. Tsai and Y. Z. Chen, *Appl. Catal., A*, 2005, **284**, 239–246.
31 B. J. Liaw, S. J. Chiang, S. W. Chen and Y. Z. Chen, *Appl. Catal., A*, 2008, **346**, 179–188.
32 L. Crowhurst, N. L. Lancaster, J. M. Pérez Arlandis and T. Welton, *J. Am. Chem. Soc.*, 2004, **126**, 11549–11555.
33 O. B. Babushkina, *Z. Naturforsch., A: Phys. Sci.*, 2008, **63**, 66–72.
34 O. B. Babushkina, S. Ekres and G. E. Nauer, *Z. Naturforsch., A: Phys. Sci.*, 2008, **63**, 73–80.
35 D. R. Kilanoqyxi, H. Teeuwen, V. H. J. De Beer, B. C. Gates, G. C. A. Schuit and H. Kwart, *J. Catal.*, 1978, **55**, 129–137.
36 M. Houalla, N. K. Nag, A. V. Sapre, D. H. Broderick and B. C. Gates, *AIChE J.*, 1978, **24**, 1015–1021.
37 T. Kabe, K. Akamatsu, A. Ishihara, S. Otsuki, M. Godo, Q. Zhang and W. Qian, *Ind. Eng. Chem. Res.*, 1997, **36**, 5146–5152.
38 P. Michaud, J. L. Lemberton and G. Perot, *Appl. Catal., A*, 1998, **169**, 343–353.
39 M. Lewandowski, A. Szymańska-Kolasa, C. Sayag, P. Beaunier and G. Djéga-Mariadassou, *Appl. Catal., B*, 2014, **144**, 750–759.
40 L. Peńa, D. Valencia and T. Klimova, *Appl. Catal., B*, 2014, **147**, 879–887.
41 Y. Okamoto, Y. Nitta, T. Imanaka and S. Teranishi, *J. Chem. Soc., Faraday Trans. 1*, 1979, **75**, 2027–2039.
42 Y. Nie, C. X. Li, A. J. Sun, H. Meng and Z. H. Wang, *Energy Fuels*, 2006, **20**, 2083–2087.
43 H. S. Gao, Y. G. Li, Y. Wu, M. F. Luo, Q. Li, J. M. Xing and H. Z. Liu, *Energy Fuels*, 2009, **23**, 2690–2694.
44 H. S. Gao, M. F. Luo, J. M. Xing, Y. Wu, Y. G. Li, W. L. Li, Q. F. Liu and H. Z. Liu, *Ind. Eng. Chem. Res.*, 2008, **47**, 8384–8388.